ROUGH SURFACES INFLUENCE ON AN INDOOR PROPAGATION SIMULATION AT 60 GHz.

Yann COCHERIL, Rodolphe VAUZELLE, Lilian AVENEAU, Majdi KHOUDEIR

SIC, FRE-CNRS 2731
Université de Poitiers - UFR SFA
Bât SP2MI - Téléport 2 - Bd Marie et Pierre Curie - BP 30179
86962 FUTUROSCOPE CHASSENEUIL CEDEX (FRANCE)

{cocheril, vauzelle, aveneau, khoudeir}@sic.sp2mi.univ-poitiers.fr

SHORT ABSTRACT

In order to propose new multimedia services, wireless telecommunication systems require an increase of bandwidth, directly connected to an increase of frequency. So, to simulate the wave propagation in indoor environments, the methods evolve. For instance, at 60 GHz, it becomes necessary to take into account new small environment details like rough surfaces. However, classical ray tracing algorithms are unusable to simulate the scattering phenomenon on rough surfaces. The objective of this paper consists of a semi-statistical description of rough surfaces in order to integrate their behaviour in a 3D ray tracing, and to study first results.
Keywords : indoor environment, 3D ray tracing, rough surfaces, scattering

1 INTRODUCTION

Nowadays, wireless telecommunication systems evolve to satisfy our growing need of multimedia services. For instance, in the case of a communication between mobiles, we want to transmit some images or videos in addition to the voice. For this reason, more and more bandwidth is necessary. To solve this problem, the working frequency of current wireless systems will increase until 60 GHz, with the coming in a more or less close future of the WLAN (Wireless Local Area Network).

To deploy such systems, the wave propagation in complex environments must be simulated. The results of those simulations enable the prediction of important channel parameters such as path loss, delay spread or coherence bandwidth. With the current systems, a wave propagation simulation based on a classical 3D ray tracing taking into account reflection, transmission and diffraction phenomena, gives sufficient results. However, with future high working frequencies, a new physical phenomenon appears : the scattering on rough surfaces. Indeed, for a propagation in indoor environments at 60 GHz, the size of surfaces roughness is close to the wavelength (λ measures $5\ mm$). Consequently, such details must be taken into account in a simulation at 60 GHz to evaluate their influence on a wave propagation.

In order to integrate the scattering phenomenon on rough surfaces in a 3D ray tracing, we use the following approach. In a first stage, a semi-statistical description is used to define rough surfaces encountered in indoor environments. It is called semi-statistical because it is based on a statistical description of the rough surfaces, parametrized thanks to deterministic informations. In a second stage, we compute the scattered power density reflected by such a rough surface. A comparison between the results of our approach and those obtained with a purely deterministic one is presented. In a third stage, a simulation based on a 3D ray tracing modified in order to take into account rough surfaces scattering phenomenon can be performed and it gives some coverage zones predictions results.

So, this paper follows this approach. Firstly, a definition of the rough surfaces is given, and our semi-statistical description is proposed in section 2. Then, a comparison between the electro-

magnetic behaviour of the semi-statistical and the deterministic descriptions of a rough surface is studied in section 3. Finally, the integration of the rough surfaces behaviour, in a 3D ray tracing, is presented, and a first result of coverage zone prediction in indoor environments at 60 GHz is shown in section 4.

2 ROUGH SURFACES

2.1 Definition

Usually, according to an incident wave (characterized by its wavelength λ and its angle of incidence ψ) on a surface, this latter can be considered smooth or rough. Indeed, if the wavelength is much more greater than the maximum difference of height h of the surface roughness (*Fig. 1*), the surface will be considered smooth. On the contrary, the surface will be considered rough if h is close to the wavelength. A criterion is used to separate these two cases.

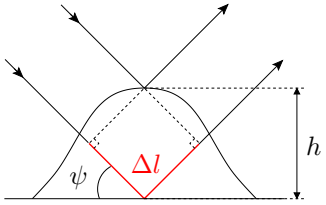

Fig. 1 : Difference of length between two paths reflected by a rough surface

It is based on the maximum difference of distance Δl existing between two rays respectively reflected by the highest and by the lowest points of a rough surface (*Fig. 1*).

$$\Delta l = 2h \sin \psi \tag{1}$$

i.e., in terms of maximum phase difference $\Delta\varphi$:

$$\Delta\varphi = \frac{2\pi}{\lambda}\Delta l = \frac{4\pi h}{\lambda} \sin \psi \tag{2}$$

If the maximum phase difference is small, the surface is considered smooth and the two rays will be almost in phase. If it increases, the two rays will interfere and the surface is considered rough. To separate these two cases, limit values of maximum phase difference have been proposed. The Rayleigh criterion [1] fixes this limit to $\Delta\varphi = \pi/2$, while the Fraunhofer criterion [2] proposes $\Delta\varphi = \pi/8$. The smaller the limit is, the smaller the roughness taken into account is. For our study, we consider the second criterion. Finally, a surface is rough if :

$$h > \frac{\lambda}{32 \sin \psi} \tag{3}$$

2.2 Surface description

In order to study the electromagnetic behaviour of rough surfaces, we have to know the geometry of their reliefs. Two different descriptions can be used, deterministic and statistical, which consists in modeling the micro-facets of rough surfaces (*Fig. 2*). Each micro-facet is characterized by its height, and its normal direction. For the statistical description [2], to perform a complete modeling of the micro-facets, three statistical laws are used. The first one manages the distribution of the heights to calculate the phase shift of a reflected ray on a micro-facet. The two other ones manage the distribution of the slopes in two orthogonal directions (x and y) to compute the reflected direction of an incident ray on a micro-facet. The three statistical laws are considered gaussian, and their means and standard deviations are arbitrarily defined.

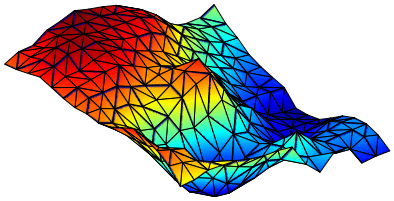

Fig. 2 : Decomposition of a rough surface with micro-facets

The deterministic description consists of an accurate knowledge of the local height of the rough surface. In our case, it is obtained with a device based on a laser sensor [4]. A map of the relief of the surface is generated (*Fig. 3*) with a sampling step equals to $80\ \mu m$ in the two horizontal dimensions and equals to $1\ \mu m$ in the vertical dimension. Each pixel of the height map, with its neighbours, define a micro-facet.
In this paper, we study particular surfaces which are different roughcasts because they are numerous in indoor environments.

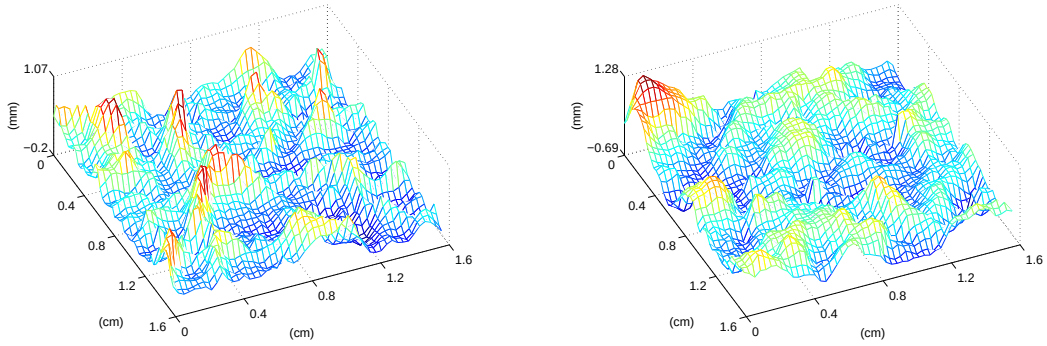

(a) height map n° 1

(b) height map n° 2

Fig. 3 : Sample of height maps of two different roughcasts

To consider a realistic description of rough surfaces, we propose a new approach associating the two previous descriptions. The statistical description described above is used and parametrized with the deterministic one. Indeed, we search from the deterministic height map the mean and the standard deviation of the three statistical laws. These estimations are based on the Kolmogorov-Smirnov test. It gives the maximum error of probability k of an estimation. Thus, for a given rough surface, we attempt to find the best couple of mean and standard deviation for each statistical law which minimizes the Kolmogorov-Smirnov test, characterized by k.
Fig. 4(a) and Fig. 4(b) show the histograms of the three laws for two different roughcasts (*Fig. 3*). The blue and red curves correspond respectively to the distributions computed with their deterministic height maps (*Fig. 3(a) and Fig. 3(b)*), and with the estimated laws according to the minimization of the Kolmogorov-Smirnov test.
From left to right, we present the results for the distribution of the slopes according to the x axis and the y axis, respectively called XS_i and YS_i, and the results for the distribution of the height called H_i (i is the number of the height map). Notice that all the averages of these statistical

laws are estimated close to 0. The standard deviation σ of the estimated laws, and the maximum probability error k ($0 < k < 1$) between these latter and the deterministic ones are presented in Tab. 1. If the deterministic description is really gaussian, $k \to 0$.

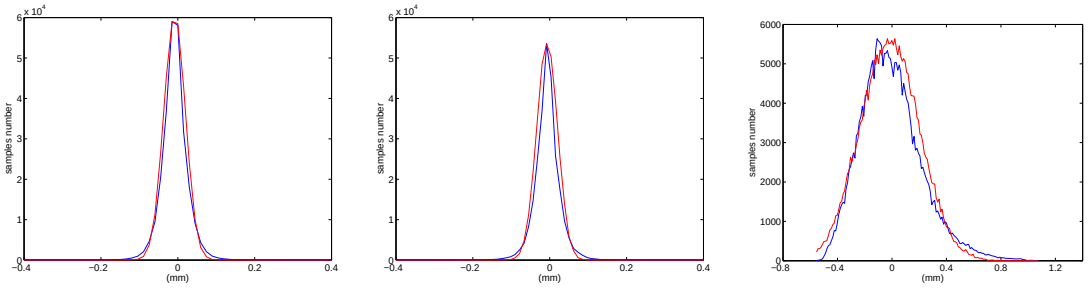

XS_1 YS_1 H_1

(a) Slope distributions according to x axis (XS_1) and y axis (YS_1), and height distribution (H_1) for surface 1

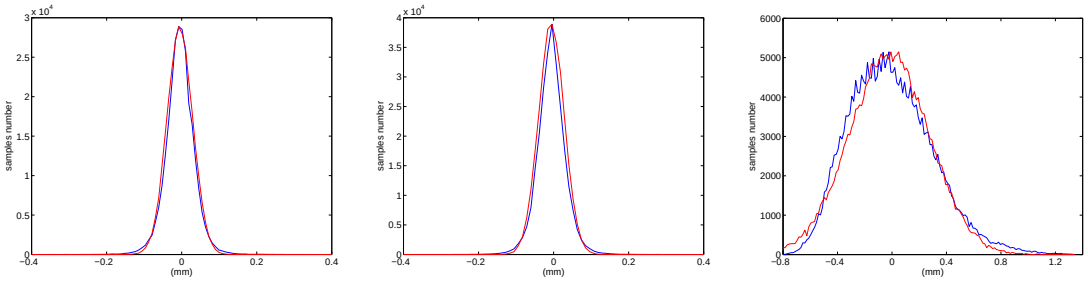

XS_2 YS_2 H_2

(b) Slope distributions according to x axis (XS_2) and y axis (YS_2), and height distribution (H_2) for surface 2

Fig. 4 : Histograms of the statistical laws of the roughcasts n° 1 (*Fig. 3(a)*) and n° 2 (*Fig. 3(b)*)

	Surface n° 1			Surface n° 2		
law	SX_1	SY_1	H_1	SX_2	SY_2	H_2
$\sigma\ (mm)$	0.028	0.027	0.249	0.034	0.034	0.293
k	0.021	0.024	0.023	0.016	0.012	0.021

Tab. 1 : Standard deviation σ and maximum probability error k of estimation for the different laws

The histograms show that the semi-statistical description is different from the deterministic one. For the rough surface 1, the maximum errors k are the same for each distribution. It comes from a skewness repartition between the low and high height values. Indeed, the slopes are calculated from the height difference of the map. A more symmetrical repartition of the heights leads to an accurate estimation of the distribution of the slopes as it is shown for the surface n° 2 ($k_{SX_2} < k_{SX_1}$ and $k_{SY_2} < k_{SY_1}$).

3 ELECTROMAGNETIC BEHAVIOUR MODELING OF ROUGH SURFACES

In order to compare the deterministic and the semi-statistical descriptions of a rough surface, we compute their reflected power densities *(4)*. To play this part, each micro-facet is treated independently. Thus,

each one receives a ray and reflects it in its own specular direction, defined by the incident ray and by the normal to the micro-facet (*Fig. 5*).

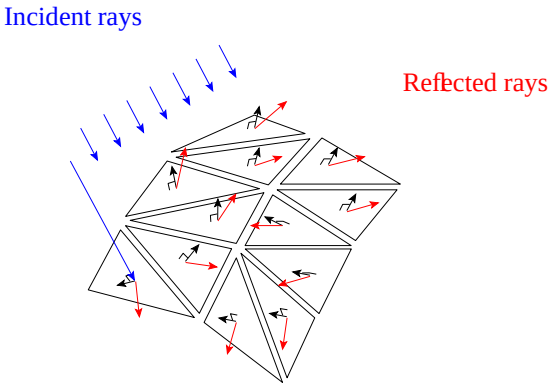

Fig. 5 : Independent behaviour of each micro-facet

Then we can apply the modified Fresnel coefficient $R_{||,\perp}^{mod}$ *(5)* on the reflected ray to compute the corresponding power density. By integrating results for all micro-facets of the surface, we can compute the total reflected power density associated to an incident wave and a surface.

$$P = |E_{||,\perp}^{i}(Q) \times R_{||,\perp}^{mod} \times e^{-2\pi jkS_r}|^2 \tag{4}$$

P represents the power density of an incident wave field $E_{||,\perp}^{i}(Q)$ at the reflection point Q, S_r away from the receiver.
with :

$$R_{||,\perp}^{mod} = R_{||,\perp} \times \rho \tag{5}$$

$$\rho = e^{-8\pi^2\left(\frac{\sigma_h}{\lambda}\right)^2 \cos^2\theta} \tag{6}$$

where $R_{||,\perp}$, ρ, σ_h, and θ represent respectively the specular Fresnel reflection coefficient, the scattering coefficient, the standard deviation of the height distribution and the incidence angle with the normal to the surface.
According to this principle, two different types of results are computed. The first one is the histogram of the reflected rays directions (*Fig. 6(a) and Fig. 7(a)*), represented in spherical coordinates. This kind of representation well shows the repartition of the reflected rays in a 3D space, i.e. the influence of the orientation of the micro-facets. The second one is the reflected power density (*Fig. 6(b) and Fig. 7(b)*). It is displayed according to the azimuth angle θ for the x axes, and the elevation angle ϕ for the y axes. To compare the reflected power densities for the deterministic and the semi-statistical descriptions, we use a criterion which characterizes their dispersions at 50% and 75% from their maximum values. Each threshold corresponds to the dispersion D_θ of the azimuth angle and the dispersion D_ϕ of the elevation angle of the reflected power densities.
Notice that only one simulation is made for the deterministic description, while one hundred are necessary for the semi-statistical one in order to have a sufficient statistic. So, we calculated the means ($m_{D_{\theta,\phi}}$) and standard deviations ($\sigma_{D_{\theta,\phi}}$) of the corresponding dispersions. The results of these two approaches are presented in Tab. 2. Fig. 6 and Fig. 7 show respectively the results for the surface n° 1 (*Fig. 3(a)*) and for the surface n° 2 (*Fig. 3(b)*), according to two different incidence angles θ.
We can see on both representations in Fig. 6 and Fig. 7 that the reflected power density of the semi-statistical model of the rough surface n° 2 well estimates the deterministic one, while the results for the rough surface n° 1 are really different. For instance, the results of dispersion for the incidence angle $\theta = 30°$ are shown in Tab. 2. Closer the dispersions values of the deterministic description (D_θ and D_ϕ) with the semi-statistical one (m_{D_θ} and m_{D_ϕ}) are, better the estimation of the three statistical laws is. The values of dispersion according to the elevation angle ϕ are always similar, so we study only the

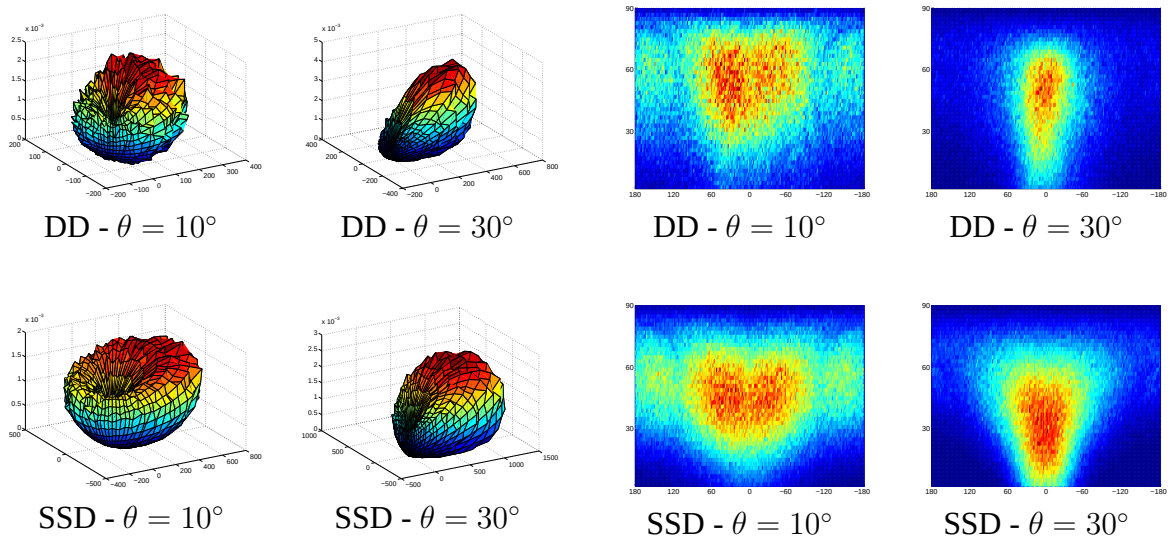

(a) Histograms of the reflected rays directions

(b) Reflected power density

Fig. 6 : Simulation results for the deterministic (DD) and the semi-statistical descriptions (SSD) for the rough surface n° 1 (*Fig. 3(a)*) for $\theta = 10°$ and $\theta = 30°$

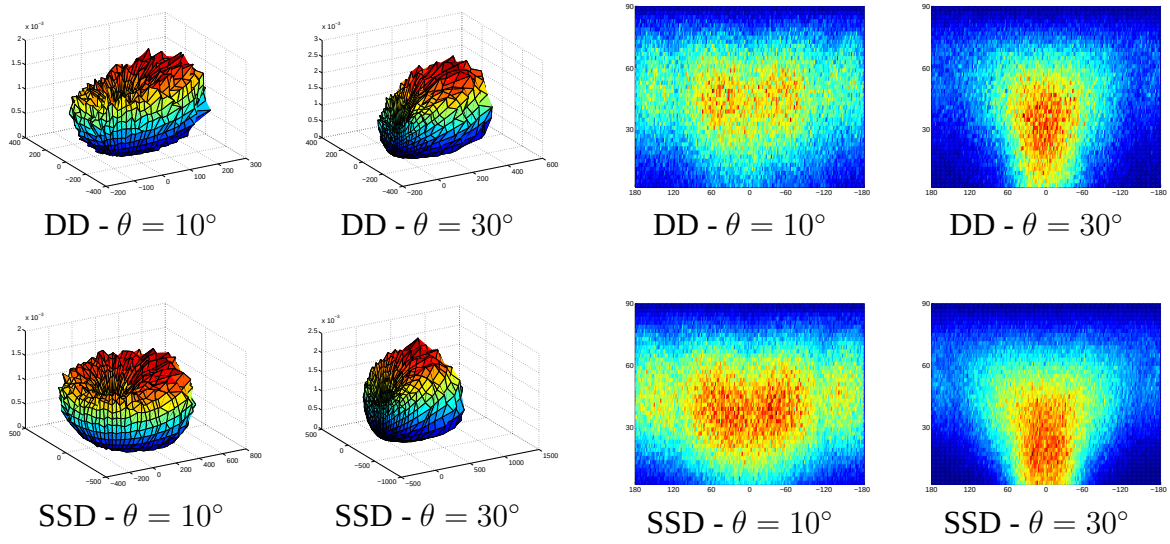

(a) Histograms of the reflected rays directions

(b) Reflected power density

Fig. 7 : Simulation results for the deterministic (DD) and the semi-statistical descriptions (SSD) for the rough surface n° 2 (*Fig. 3(b)*) for $\theta = 10°$ and $\theta = 30°$

values of dispersions according to the azimuth angle θ. On the one hand, the dispersions obtained for the semi-statistical description for the rough surface n° 2 are close to the deterministic ones (for instance $D_\theta = 224°$ and $m_{D_\theta} = 229.6°$ with $\sigma_{D_\theta} = 22.6°$); on the other hand, the results obtained for the rough surface n° 1 not suit well the deterministic ones (for instance $D_\theta = 111°$ while $m_{D_\theta} = 164°$ with $\sigma_{D_\theta} = 19.7°$). As we saw in the last section, the slope distributions for the rough surface n° 2

	Surface n° 1				Surface n° 2			
Deterministic	D_θ		D_ϕ		D_θ		D_ϕ	
$T_{50\%}$	$111°$		$65°$		$224°$		$67°$	
$T_{75\%}$	$71°$		$34°$		$104°$		$45°$	
Semi-statistical	m_{D_θ}	σ_{D_θ}	m_{D_ϕ}	σ_{D_ϕ}	m_{D_θ}	σ_{D_θ}	m_{D_ϕ}	σ_{D_ϕ}
$T_{50\%}$	$164.0°$	$19.7°$	$65.5°$	$1.6°$	$229.6°$	$22.6°$	$64.4°$	$2.3°$
$T_{75\%}$	$80.83°$	$13.73°$	$41.78°$	$5.95°$	$118.65°$	$21.49°$	$47.11°$	$5.13°$

Tab. 2 : Dispersion measurements for the deterministic and the semi-statistical descriptions ($\theta = 30°$)

have a more accurate estimation than the ones of the rough surface n° 1 (*Tab. 1*). So, we can conclude that with a good accuracy of the slope distributions, the semi-statistical representation becomes closer to the deterministic one. Notice that the accuracy of the height distribution is similar, so that we can not conclude on their influence on the results.
Finally, the electromagnetic behaviour is very sensitive to the variations of the distributions parameters. So, our semi-statistical description of the rough surfaces studied is very interesting in order to have a realistic simulation of the scattering phenomenon.

4 INTEGRATION IN A RAY TRACING AND RESULTS

In order to study the influence of the rough surfaces on a transmission at 60 GHz in an indoor environment, we have integrated the previous approach in a wave propagation model based on a 3D ray tracing [3].
Recall that a classical ray tracing computes all the existing paths between a transmitter and a receiver according to an allowed number of propagation phenomena like reflection, transmission and diffraction. The use of a description of the surfaces based on micro-facets is incompatible with a classical ray tracing. Indeed, to simulate the electromagnetic behaviour of a rough surface it must be hit by a great number of rays. It is not the case in a classical ray tracing, so we have to modify it.

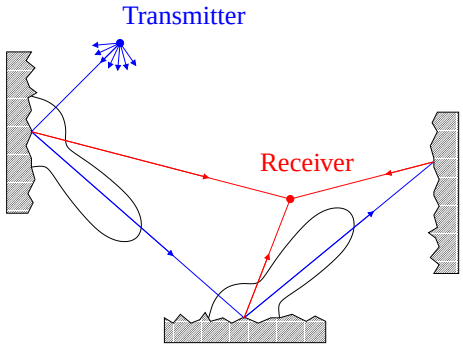

Fig. 8 : Principle of path tracing for three reflections

We apply a method used in the image synthesis field named path tracing, based on Monte-Carlo methods. Each surface is defined by its roughness properties estimated with the method proposed in the section 2.2. From the transmitter, we send a great number of rays in random directions and let propagate them until an allowed number of interactions with the surfaces of the environment. We search the intersection of a ray with these latter. If it exists, we test the visibility between the intersected point and the receiver. In the positive case, we link these points (see Fig. 8 for an example with three reflections) with a ray which its magnitude is computed using the equation *(5)* and using the probability to have a reflected ray

in this particular direction (calculated according to the slope distributions of the surfaces). If the number of reflections allowed is greater than one, the process continues recursively. Then, each intersected rough surface generates one or more rays according to its own statistical laws.
In practice, we have made two different simulations. The first one is realized with the classical ray tracing technique, considering smooth surfaces (*Fig. 9(a)*). The second one is performed with our modified ray tracing technique, considering all the same rough surfaces (*Fig. 9(b)*). For these simulations, we compute the coverage zone prediction in a square room environment, with an interaction level set to two reflections.

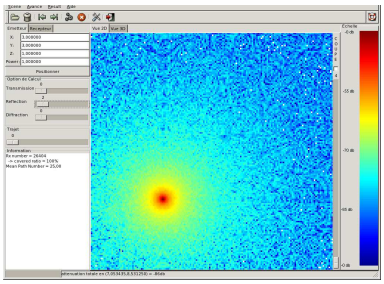

(a) Classical ray tracing with smooth surfaces for two reflections

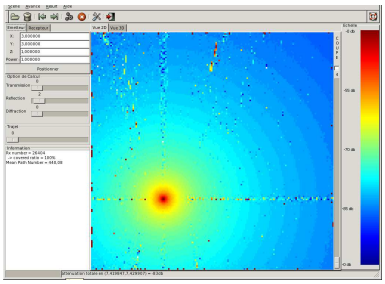

(b) Modified ray tracing with rough surfaces for two reflections

Fig. 9 : Coverage zones predictions for a square room composed with smooth or rough surfaces

We can see that the rough surfaces have a significant effect on the simulation results. The electromagnetic behaviours, seen in section 3, of each rough surface lead to a smoother coverage zone. Indeed, the interference phenomena are canceled because, in the modified ray tracing, each position of the receiver is reached by a great number of rays, randomly reflected by the rough surfaces.

5 CONCLUSION

To study the influence of the surfaces roughness on the wave propagation in an indoor environment, we developed a new approach based on a semi-statistical description of the rough surfaces and modified a 3D ray tracing in order to integrate them. A first version of this modified ray tracing is available. The obtained results show a difference between simulations in a smooth or rough environments. So, to complete these first results, we have to make a parametric study. Wave propagation in several indoor environments composed with different size of surfaces roughness have to be simulated. Furthermore, we have to determine the influence of parameters such as the number of rays emitted from the transmitter or the number of ray emitted from each hit point. Finally, to characterize the channel propagation, the impulse response have to be computed.

References

[1] P. Beckmann and A. Spizzichino. *The Scattering of Electromagnetic Waves from Rough Surfaces*. Pergamon, 1963.

[2] Dirk Didascalou, Martin Dottling, Norbert Geng, and Werner Wiesbeck. An approach to include stochastic rough surface scattering into deterministic ray-optical wave propagation modeling. *IEEE Trans. on Antennas and Prop.*, 51(7):1508–1515, July 2003.

[3] F. Escarieu, Y. Pousset, R. Vauzelle, and L. Aveneau. Outdoor and indoor channel characterization by a 3d simulation software. In *IEEE PIRMC'2001*, San Diego, Oct 2001. 5 pages (CD-ROM).

[4] H. Zahouani, R. Vargiolu, and M.T. Do. Characterization of microtexture related to wet road/tire friction. *AIPCR/PIARC*, pages 195–205, June 2000.